

Eutectic cell and nodule count as the quality factors of cast iron

E. Fraś*, M. Górny

AGH University of Science and Technology, Reymonta 23 Str., 30-059 Kraków, Poland

* Corresponding author. E-mail address: edfras@agh.edu.pl

Received 16.04.2008; accepted in revised form 29.04.2008

Abstract

In this work the predictions based on a theoretical analysis aimed at elucidating of eutectic cell count or nodule counts N were experimentally verified. The experimental work was focused on processing flake graphite and ductile iron under various inoculation conditions in order to achieve various physicochemical states of the experimental melts. In addition, plates of various wall thicknesses, s were cast and the resultant eutectic cell or nodule counts were established. Moreover, thermal analysis was used to find out the degree of maximum undercooling for the graphite eutectic, ΔT_m . A relationship was found between the eutectic cell or nodule count and the maximum undercooling ΔT_m . In addition it was also found that N can be related to the wall thickness of plate shaped castings. Finally, the present work provides a rationale for the effect of technological factors such as the melt chemistry, inoculation practice, and holding temperature and time on the resultant cell count or nodule count of cast iron. In particular, good agreement was found between the predictions of the theoretical analysis and the experimental data.

Keywords: Gray cast iron; Ductile iron; Eutectic cell count; Nodule count

1. Introduction

In gray cast iron the austenite-graphite eutectic solidification process is concomitant with the formation of eutectic cells that are more or less spherical in shape (Fig.1a,b). These eutectic cells consist of interconnected graphite plates surrounded by austenite. It is generally believed that each eutectic cell is the product of a graphite nucleation event, hence the cell count can be a measure of the graphite nucleation susceptibility. In general, by increasing the eutectic cell count; (a) the strength of cast iron increases (through a reduction in ferrite and an increase in graphite type A) [1], (b) the chill of cast iron is reduced [2] and (c) the pre-shrinkage expansion increases [3,4] and in consequence the probability of developing unsoundness in castings.

In ductile iron each graphite nucleus gives rise to a single graphite nodule (Fig.1d,e), thus nucleation establishes the final nodule count. Accordingly, by increasing the nodule count in cast iron leads to: (a) increasing strength and ductility in ADI iron [5] and improved microstructural homogeneity [6,7], (b) reduction in the chilling tendency of cast iron [8,9], increasing pre-shrinkage expansion [3], and increasing fraction of ferrite in the microstructure [10].

Accordingly, it can be affirmed that graphite eutectic cells or nodules play a significant role in the exhibited properties becoming important factors in the foundry practice. Thus, the purpose of this work is to account for the effect of the different physical and technological parameters on the exhibited cell and nodule count in cast iron, from the point of view of a theoretical analysis, and its experimental verification.

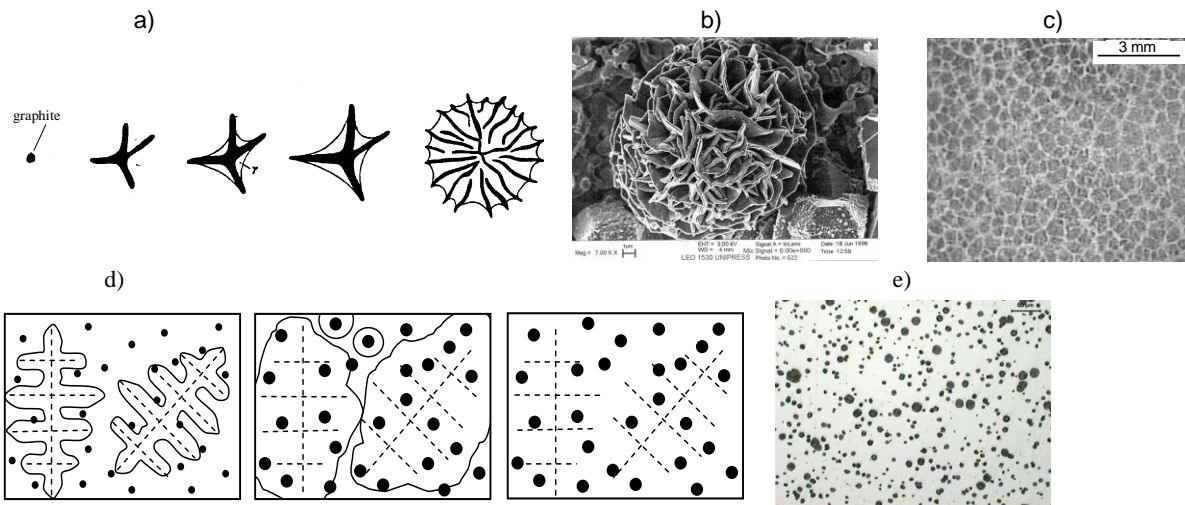


Fig. 1. Illustration of (a) the development of eutectic graphite- austenite cells during solidification of flake graphite cast iron, (b) eutectic cell, (c) graphite eutectic cell boundaries, etched with Stead reagent, (d), graphic depiction of solidification of ductile iron, and (e) structure of ductile iron

2. Experimental procedure

2.1. Flake graphite cast iron

Experimental melts were made in a electric induction furnace containing a 15 kg capacity crucible. The raw materials were pig iron, steel scrap, commercially pure silicon, and Fe-P, Fe-S alloys. Melting was followed by liquid iron superheating up to 1420°C and inoculation using FOUNDRYSIL with a 0.2 - 0.5 cm granulation, and added as 0.5 % of the total charge weight. After various time intervals (1.5, 5, 10, 15, 20 and 25 minutes) from the instant of inoculation, the cast iron was poured into plate shaped molds of $s = 0.6$; $s = 1.0$; $s = 1.6$; $s = 2.2$ and $s = 3.0$ cm in thickness. The average chemical composition of the cast iron was : C =3.18%, Si =1.91%, Mn = 0.13%, P = 0.092%, S = 0.064%. In all the cases, the plates had a common gating system. The foundry molds were prepared using conventional molding sand. In addition, they were instrumented with Pt/PtRh10 thermocouples enclosed in quartz sleeves. The thermocouple tips were placed in the geometrical center of each mold cavity. An Agilent 34970A electronic module was employed for recording the cooling curves used for determinations of the initial metal temperature T_i just after filling of mold, as well as the maximum undercooling, ΔT_m at the onset of eutectic solidification. After cooling, specimens for metallographic examination were taken from the geometrical plate centers. Metallographic examinations were made on polished and etched (Stead reagent) specimens to reveal the graphite eutectic cell boundaries. The planar microstructure is characterized by the average number of eutectic cells N_F per unit area (cell count) [11]

$$N_F = \frac{N_i + 0.5 N_w + 1}{F} \quad (1)$$

where N_i is the number of eutectic cells inside the rectangle S , N_w is the number of eutectic cells that intersect the sides of S but not their corners and F is the surface area of S .

The average number of eutectic cells N per unit volume (volumetric cell count) is given by [12]

$$N \cong 0.568 (N_F)^{3/2} \quad (2)$$

2.2. Ductile iron

The test melts were made in an electric induction furnace of 8000 kg capacity. The raw materials employed were nodular and steel scrap and commercially pure silicon. After melting and preheating at 1485°C, cast iron was poured into a casting ladle where it was spheroidized using the cored wired injection method. Different inoculants in various amounts were used. The aim of using different inoculants and inoculation processes was to induce different maximum undercooling values. The average chemical composition of nodular iron was: C =3.69%, Si =2.63%, Mn = 0.42%, P = 0.02%, S = 0.02%, Mg =0.04%. Ductile iron was poured into the same molds as for gray cast iron. Also, the experimental methods used in determining the cooling curves and the metallographic determinations were similar as for gray cast iron. In ductile iron the graphite nodules are characterized by Raleigh distributions [13] so the volumetric nodule count, N can be related to the planar nodule count N_F using the Wiencek equation [14]:

$$N = \sqrt{\frac{N_F^3}{f_{gr}}} \quad (3)$$

where f_{gr} is the volume fraction of graphite at room temperature.

3. Results and discussion

The theoretical analysis of the solidification process for cast iron shows that the volumetric cell or nodule count N in cast iron can be described [15,16] by

$$N = N_s \exp\left(-\frac{b}{\Delta T_m}\right) \quad (4)$$

Moreover, from published works [17,18], expressions for N are given by

- Flake graphite cast iron

$$N = \frac{N_s}{\exp\left[\text{ProductLog}(y)\right]} \quad (5)$$

- Ductile iron

$$N = \frac{N_s}{\exp\left[\text{ProductLog}(y_n)\right]} \quad (6)$$

where

$$\Delta T_m = T_s - T_m \quad (7)$$

$$y = \frac{\pi^{3/4} b}{16} \left[\frac{L_e N_s (1 - f_\gamma) c_{ef}^2 \mu^3 \phi^3 s^6}{8 a^6 T_s^3} \right]^{1/8} \quad (8)$$

$$y_n = \frac{b c}{4} \left(\frac{z B L_e N_s s^3}{a^3} \right)^{1/2} \left(\frac{\pi^5 D^3 \beta^3}{T_c^3} \right)^{1/4} \quad (9)$$

$$\phi = c_{ef} B_1 + c B_2 \quad (10)$$

$$B = \ln \frac{T_i}{T_s}; \quad B_1 = \ln \frac{T_l}{T_s}, \quad B_2 = \ln \frac{T_i}{T_l} \quad (11)$$

$$c_{ef} = c + \frac{L_\gamma}{T_{l\gamma} - T_e} \quad (12)$$

$$z = 0.41 + 0.93 B \quad (13)$$

In the equations (4)-(13): N_s , and b , are the nucleation coefficients for flake graphite or ductile iron, f_γ is the volumetric fraction of austenite (see Table 1), a is the material mould ability to absorb heat, s is the wall thickness of castings, c_{ef} is the effective specific heat of proeutectic austenite, T_i is the initial metal temperature just after filling the mould, ϕ is the heat coefficient, T_m is the minimal temperature at the onset of eutectic solidification determined from the cooling curves and c , L_e , L_γ , T_s , T_l , $T_{l\gamma}$, D , β and μ are defined in Table 1. The $\text{ProductLog}[y] = x$ is the Lambert function*, is also known as the omega function which can be easily calculated by means of the instruction $\text{ProductLog}[y]$ in the Mathematica™ programme.

* see <http://mathworld.wolfram.com/LambertW-function.html>,

Table 1.
Selected thermophysical data

Parameter	Value and units
Latent heat of graphite eutectic	$L_e = 2028.8$; J/cm ³
Latent heat of austenite	$L_\gamma = 1904.4$; J/cm ³
Specific heat of cast iron	$c = 5.95$; J/(cm ³ °C)
Growth coefficient of graphite eutectic	$\mu = 10^{-6} (2 - 6.3 \text{ Si})^{0.25}$; cm/(°C ² s)
The diffusion coefficient of carbon in austenite	$D = 3.9 \cdot 10^{-6}$; cm ² /s
Coefficient related with the slopes of the solubility lines JE', ES and BC' in Fe-C system	$\beta = 0.00155$; °C ⁻¹ .
Material mould ability to absorb heat	$a = 0.10$; J/(cm ² s ^{1/2} °C)
Liquidus temperature for austenite	$T_l = 1636 - 113(C + 0.25\text{Si} + 0.5\text{P})$; °C
Formation temperature for cementite eutectic	$T_c = 1130.56 + 4.06(C - 3.33\text{Si} - 12.58\text{P})$; °C
Graphite eutectic equilibrium temperature	$T_s = 1154.0 + 5.25\text{Si} - 14.88\text{P}$; °C
Carbon content in graphite eutectic	$C_e = 4.26 - 0.30\text{Si} - 0.36\text{P}$; %
Maximum carbon content in austenite at T_s	$C_\gamma = 2.08 - 0.11\text{Si} - .35\text{P}$; %
Liquidus temperature of austenite for austenite composition C_γ	$T_{l\gamma} = 1636 - 113(2.08 + 0.15\text{Si} + 0.14\text{P})$; °C
Weight fraction of austenite	$g_\gamma = (C_e - C)/(C_e - C_\gamma)$
Austenite density	$\rho_\gamma = 7.51$ g/cm ³
Melt density	$\rho_m = 7.1$ g/cm ³
Volume fraction of proeutectic austenite	$f_\gamma = \rho_m g_\gamma / [\rho_\gamma + g_\gamma (\rho_m - \rho_\gamma)]$

Considering the experimental outcome ΔT_m and N , as well as Eq. (4), nucleation coefficients, N_s and b (which determine the respective melt nucleation susceptibilities for graphite) can be obtained using statistical methods (Table 2). In these calculations the correlation coefficients are relatively high (Table 2) suggesting that in each case, the relationships between N and ΔT_m described by Eq. (4) are in good agreement with the experimental outcome.

From Table 1 and the nucleation parameters, N_s and b given in Table. 2 for the average chemical composition of the cast irons, calculations were made of the effect of wall thickness on the cell or nodule count by considering Eqs. (5) and (6). Accordingly, the results from these calculations are shown in Fig. 2 in solid lines. Also, for comparison purposes the experimental results are included in this figure. Once again, notice that there is good agreement between the experimental outcome and the predictions of the proposed theoretical analysis.

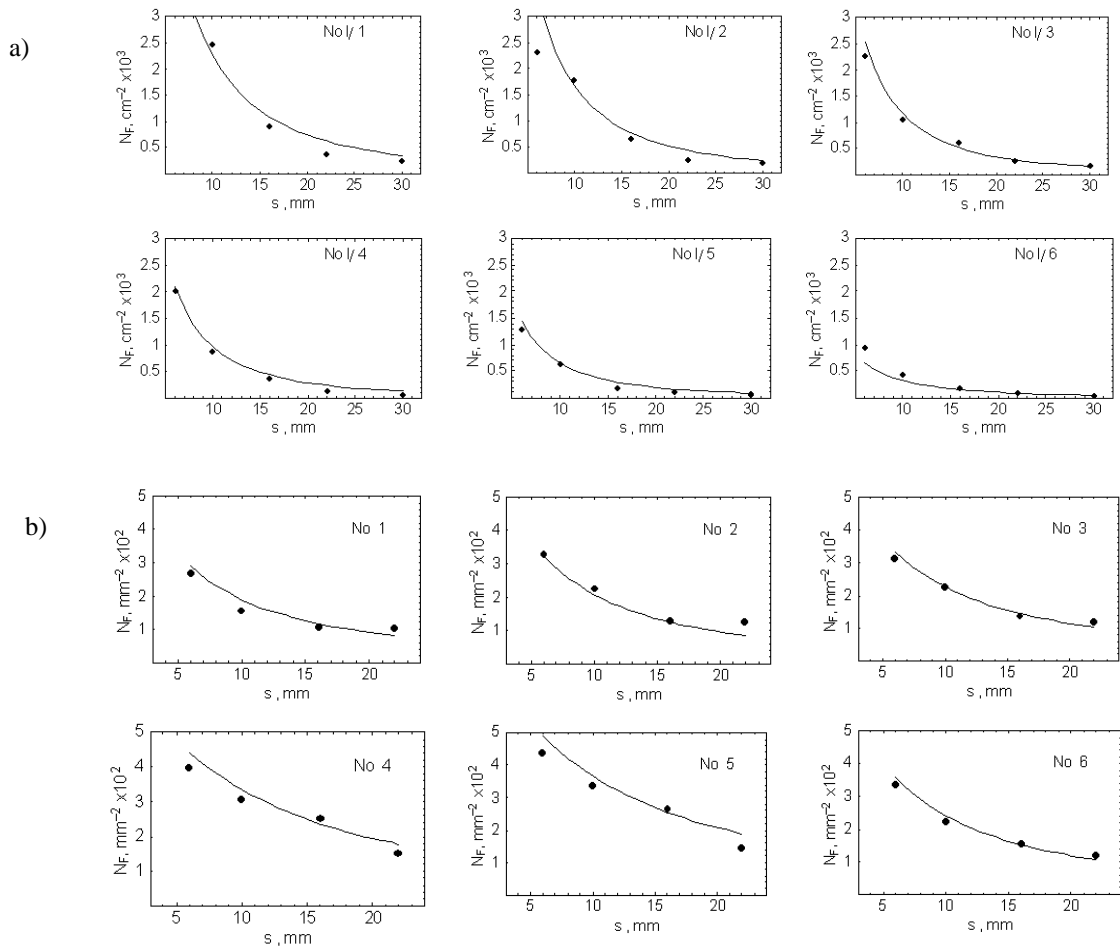


Fig. 2. Influence of the wall thickness on the cell (a) and nodule count (b); points - experimental results, lines - results based on Eqs.(5) and (6)

From Eqs. (5)-(13) it can be seen that among the various factors that influence the eutectic cell or nodule count are:

- *Nucleation susceptibilities of graphite* are characterized by the N_s and b coefficients. Depending on the N_s and b values, at a given cooling rate, various cells or nodule count can be achieved in cast iron. These coefficients depend on the chemical composition, inoculation practice, bath holding times and temperatures. In general, from Eqs. (5), (6), (8) and (9), it is apparent that the cell or nodule count increases when b decreases and N_s increases. The effect of the chemical composition of cast iron on N_s and b is not considered in this work as there is not enough information available in the literature. For flake graphite inoculated cast iron (Table 2) the nucleation coefficients N_s and b can be related with a dimensionless time $t_d = t / t_r$ (where t is the time calculated from the instant in which the inoculant was introduced into the melt and t_r is the time when the observed changes in the cell count are negligible ($t_r = 25$ minutes)).

$$N_s = 10^6 (5.5 - 0.8 t_d - 5.3 t_d^2); \quad [\text{cm}^{-3}] \quad ,$$

$$b = 96.9 + 122.6 t_d - 59.2 t_d^2; \quad [^\circ\text{C}] \quad (14)$$

Prolonged bath holding times lead to a reduction in N_s and to an increase in b . However, the effect of a reduction of N_s is prevalent and as result prolonged bath holding times lead to a reduction in the cell count.

- *The graphite eutectic growth coefficient μ* . In flake graphite cast iron it depends on the silicon content in cast iron (see Table 1). In general, Si lowers the eutectic growth coefficient, so according to Eqs. (5) and (8) as the Si content increases the cell count in the cast iron also increases.

- *The effect of the volumetric fraction of austenite f_γ* (in flake graphite cast iron). The volumetric fraction is described by the expressions given in Table 1. From these expressions, it is

found that by increasing the amount of carbon and silicon the volume fraction of austenite is lowered, thus according to Eqs. (5) and (8) decreasing the cell count.

- *The effect of the liquidus temperature T_l .* The liquidus temperature is given by the equation in Table 1. It is found that by increasing the amount of carbon and silicon the T_l is lowered, thus according to Eqs. (5) and (8) increasing the cell count.

- *The β coefficient* can be assumed as constant.

- *The diffusion coefficient of carbon in austenite D .* In general, in ductile iron as D increases, the nodule count decreases as predicted by Eqs. (6) and (9). Moreover, D depends on the actual temperature and chemical composition of the austenite. The effect of Si, Mn and P on D is not considered in this work as there is not enough information available in the literature. During the eutectic transformation, the temperature, T ranges approx. from 1100 to 1150°C, so the effective D values range from 3.2×10^{-6} to $4.6 \times 10^{-6} \text{ cm}^2/\text{s}$ [19]. Thus, an average D value of $3.9 \times 10^{-6} \text{ cm}^2/\text{s}$ can be used without introducing significant error (Table 1).

- *The effect of the carbon equivalent CE .* Influence of $CE = C + 0.33 \text{ Si}$ on eutectic cells or nodule count is expressed in Eqs. (5) and (6) indirectly by effect of cast iron chemical composition on N_s , b , D , μ , T_l , T_l/γ , f_γ and T_s . In general, it is known that eutectic cell in base cast iron or nodule count of ductile cast iron N increases while in inoculated cast iron decreases with increasing of the carbon equivalent (Fig.3).

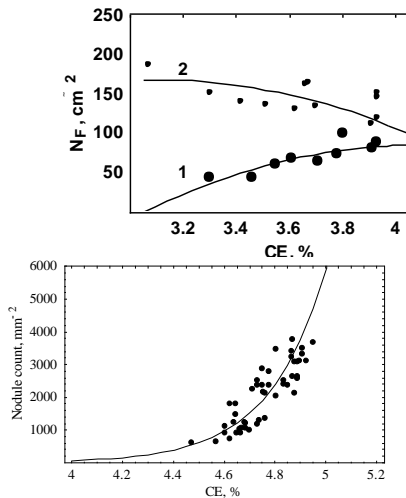


Fig. 3. Effect of carbon equivalent ($CE = C + 0.33 \text{ Si}$) on eutectic cell count; curve 1 base cast iron, curve 2 inoculated cast iron [20] (a) and on nodule count [8] (b)

- *Parameters influencing the cooling rate, Q of liquid cast iron at the temperature T_s .*

$$\text{flake graphite cast iron: } Q = \frac{8 T_s a^2}{\pi \phi c_{ef} s^2} \quad \text{ductile}$$

$$\text{iron: } Q = \frac{8 T_s a^2}{\pi B c^2 s^2} \quad (15)$$

According to Eqs. (5), (8) and (6), (9) the cell and nodule count increases as the mold ability to absorb heat, a increases and as the wall thickness, s decreases. The cell and nodule count is also dependent on the B , B_1 , B_2 , ϕ and z parameters (Eqs. (10),(11) and (13)), and hence on the initial temperature T_i of the cast iron just after pouring into the mold). The higher the pouring temperature, T_p the higher T_i . Hence, decreasing T_p temperature lowers the ϕ parameter, thus increasing the cell or nodule count. A schematic diagram showing the role of the various technological factors on the cell and nodule count in cast iron is given in Fig.4.

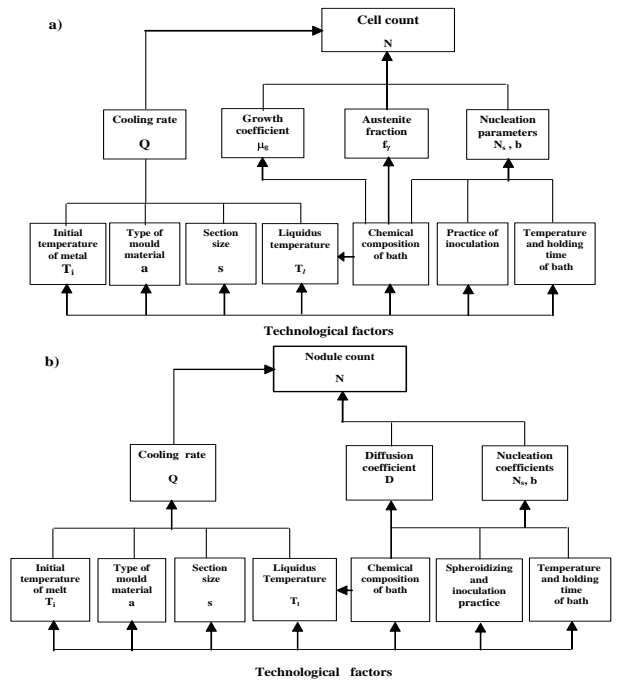


Fig. 4. Schematic representation of the effect of various technological factors on the eutectic cell count (a) and nodule count (b)

4. Conclusions

1. Novel expressions are presented for the cell and nodule count of cast iron. This work gives a description of the effects of various factors of technological importance on the cell or nodule count of cast iron. In particular, the present analysis for the cell or nodule count of cast iron indicates that they depend on:

- The chemical composition of the cast iron (through N_s , b , f_γ , D , T_l and μ).
- The inoculation and spheroidizing practice, bath superheating temperature and holding time (through N_s , b).
- Cooling rate, (through s , a , T_i and T_l).

2. Theoretical calculations were made and then compared with the experimental results on cell and nodule count and with the maximum undercooling ΔT_m at the onset of graphite eutectic

solidification (Eq. (4)) as well as with the wall thickness s (Eqs. (5)-(8)). It was found that the predictions of the theoretical analysis are in good agreement with the experimental outcome.

References

- [1] E. Fraś, C. Podrzucki, Inoculated Cast Iron, AGH, Cracow, 1978.
- [2] E. Fraś, H.Lopez, Acta Metallurgica and Materialia , 1993, vol. 41, no.12, p.3575.
- [3] E. Fraś, H.Lopez, AFS Transactions, 1994, p. 597.
- [4] H. Morrogh, Journal of The Iron and Steel Institute, January, 1968, p.1.
- [5] Liu Jincheng, R. Elliot, International Journal of Cast Metals Researches, 1999, vol.11, p. 407.
- [6] G.Lesoult, M. Castro, J. Lacaze, Acta Materialia, 1999, vol. 47, p. 3779.
- [7] M.N. Achmadabadi, E. Niyama, T. Ohide, AFS Transactions, 1994, p. 269.
- [8] A. Javaid, J.Thompson, K.G. Davis, AFS Transactions, 2002, p. 889.
- [9] A. Javaid, J. Thompson, M. Sahoo, K.G. Davis, AFS Transactions 1999, p. 441.
- [10] D. Venugopalan, Metallurgical and Materials Transactions, 1990, vol. 21 A, p. 913.
- [11] J. Rys, Stereology of materials, Fotobit, Cracow, 1995.
- [12] J. Osher, Lorz.: Quantitative Gefuengenanalyse, DVG, Leipzig-Stuttgart, 1994.
- [13] L. Wojnar, Acta Stereologica, 1986, vol. 5/2, p. 319.
- [14] K. Wiencek, J. Rys , Materialas Engineering, 1998, No.3, p.396.
- [15] E. Fraś, M. Gorny, H. Lopez International Journal of Cast Metals Researches, 2005,vol.18, p.156.
- [16] E.Fraś, M.Gorny , J.Tartera, International Journal of Cast Research, 2003, vol.16, p. 99.
- [17] E. Fraś, M. Gorny, H. Lopez, Metallurgy and Foundry Engineering, 2005,vol.31, no.2, p.137.
- [18] E. Fraś, M. Gorny, H. Lopez, Metallurgical and Materials Transactions A, 2005, vol.36A, p.3075.
- [19] J. Agren, Scripta Matallurgica, 1986, vol. 20, p.1507.
- [20] H.D. Merchant, L.J. Torriello, J.F.Wallace. Transaction of AFS, 1963, p.882.